Ageing Mechanism of Gold and Silver Nanorods in Aqueous Solution

D. Segets[*], C. Damm[*], B. Vieweg[**], G. Yang[**], E. Spiecker[**] and W. Peukert[*]

[*]Institute of Particle Technology, FAU Erlangen-Nuremberg
Cauerstr. 4, D-91058 Erlangen, Germany, D.Segets@lfg.uni-erlangen.de
[**]Department of Materials Science and Engineering, WW7, FAU Erlangen-Nuremberg
Cauerstr. 6, D-91058 Erlangen, Germany, Erdmann.Spiecker@ww.de

ABSTRACT

The current work addresses the understanding of the shape transformation of silver and gold nanorods towards more spherical nanostructures in aqueous suspension at ambient temperature. The shape transformation process was characterised using UV/Vis absorption spectroscopy, scanning electron microscopy (SEM), anodic stripping voltammetry and high resolution transmission electron microscopy (HRTEM). The increase in the particle number density during ageing indicates that the rods break spontaneously in smaller particles by surface defect induced ripening.

Keywords: silver nanorods, gold nanorods, optical characterization, ageing, shape stability

1 INTRODUCTION

Optical properties of noble metal nanoparticles including gold or silver strongly depend on particle size and shape.[1] Triggered by their interesting plasmonic properties, an increasing number of synthesis routes are leading to nanorods, nanowires and platelets, as it was recently reported in the literature.[2] These anisotropic particles typically show defective crystal stuctures.[3] Due to their face-centered cubic (fcc) crystal lattice, the equilibrium shape of noble metals usually is close to spherical. Thus, strongly anisotropic shapes may be thermodynamically unstable. Therefore, the long-term stabilization of rods and wires should be addressed in dependency of the related defects. In comparison to the well-known stabilization of spherical nanoparticles against agglomeration,[4] shape stability is a comparatively new field which is addressed in the following.

2 EXPERIMENTAL

2.1 Materials and nanoparticle preparation

The silver and gold nanorods were prepared by reduction of silver nitrate and chloro gold(III)-acid, respectively, in CTAB micelles in the presence of seed particles.[2c-e, 5] The glassware used for every particle synthesis was carefully rinsed with Millipore water prior to use. For the preparation of silver seed particles 0.25 ml of a 0.01 molar aqueous solution of silver nitrate were mixed with 8.9 ml of water. To this solution 0.25 ml of a 0.01 molar aqueous solution of trisodium citrate and 0.3 ml of a freshly prepared ice-cold 0.01 molar aqueous solution of sodium borohydride were added under vigorous stirring for 1 min. The seed particles have been stored at ambient temperature for 2 h prior to use. For the preparation of silver nanorods 0.25 ml of a 0.01 molar aqueous solution of silver nitrate were added to 10 ml of a 0.1 molar aqueous CTAB solution. To this solution 0.5 ml of a 0.1 molar aqueous solution of ascorbic acid and 0.25 ml of the silver seed suspension were added under gently shaking. Finally, 0.1 ml of a 1 molar sodium hydroxide solution was added to this solution resulting in the formation of sodium ascorbate acting as a reducing agent for silver ions. 10 min after addition of the sodium hydroxide solution the silver particles were purified by centrifugation (6.000 rpm, 30 minutes) and subsequent washing two times with Millipore water.

For the preparation of gold seed particles 0.2 ml of a 0.01 molar aqueous solution of chloro gold(III)-acid were mixed with 7.5 ml of a 0.1 molar aqueous CTAB solution. To this solution 0.6 ml of a freshly prepared ice-cold 0.01 molar aqueous solution of sodium borohydride were added under vigorous stirring for 1 min. The seed particles have been stored at ambient temperature for 2 h prior to use. For the preparation of gold nanorods 0.4 ml of 0.01 molar aqueous chloro gold(III)-acid were added to 9.5 ml of a 0.1 molar aqueous CTAB solution. To this solution 60 µl of a 0.01 molar aqueous silver nitrate solution and 64 µl of a 0.1 molar aqueous solution of ascorbic acid were added under gently shaking. After addition of the ascorbic acid solution the brownish solution became colourless because the Au(III) ions are reduced to Au(I). Finally, 8.5 µl of the gold seed suspension were

added to this solution resulting in reduction of Au(I) ions to rod-like gold nanoparticles. The suspension of the gold nanorods was stored at ambient temperature for 1 h and purified by centrifugation (14.000 rpm, 10 min) and washing two times with Millipore water.

2.2 UV/Vis absorption spectroscopy

The extinction spectra of the suspensions of the silver nanorods were recorded in the range from 900 nm to 300 nm using a UV/Vis absorption spectrophotometer "Cary 100 Scan" (Varian). Disposable PMMA cuvettes (optical path: 1 cm) were used for absorption spectroscopy.

2.3 Anodic stripping voltammetry

A device consisting of a glassy carbon working electrode, a silver/silver chloride reference electrode and a platinum wire counter electrode supplied by Metrohm was used for anodic stripping voltammetry experiments. The electrolyte was a 0.1 M aqueous KNO_3 solution.

2.4 Electron microscopy

A scanning electron microscope (SEM) "Gemini Ultra 55" (Zeiss) was used to investigate the morphology of the silver nanoparticles. For the preparation of samples for SEM-investigation one droplet of the suspension of the nanoparticles was deposited onto a silicon wafer. The coated wafers were dried at ambient temperature.

Additionally, the shape transformation was investigated using a transmission electron microscope (TEM) "CM 300 LaB6/Ultratwin" (Philips). For the measurement 7 µl of suspension were deposited onto a carbon-coated copper grid and dried at ambient temperature.

3 RESULTS AND DISCUSSION

3.1 Stability of rod-like nanoparticles

Figure 1 shows the SEM micrographs of the silver nanorods immediately after synthesis (A), after 2 h (B), 24 h (C) and after 17 days (C) of ageing at 25 °C.

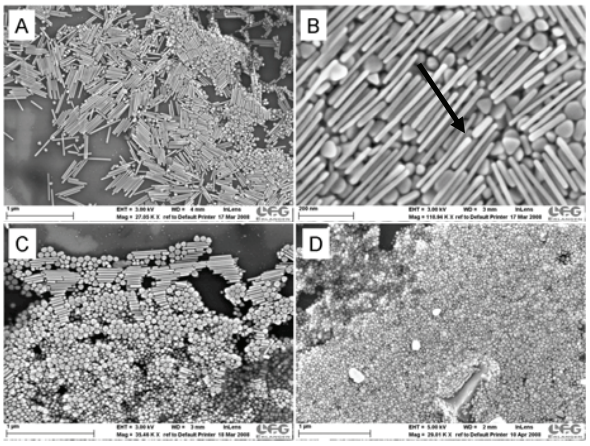

Figure 1: SEM micrographs of silver nanorods immediately after synthesis (A), after 2 h of ageing at 25 °C (B), after 24 h of ageing at 25 °C (C) and after 17 days of ageing at 25 °C (D), respectively.

It can be observed that the nanorods become shorter and significantly thicker with time and that the amount of spherical nanoparticles increases significantly. Moreover, as the optical properties of silver nanoparticles depend strongly on their size and shape, the ageing can also be observed by UV/Vis absorption spectroscopy. Regarding the extinction spectrum measured immediately after synthesis, two peaks are observed. One peak around 495 nm which refers to the longitudinal surface plasmon resonance (SPR) and one at 415 nm which refers to the transverse SPR of the initial rods.

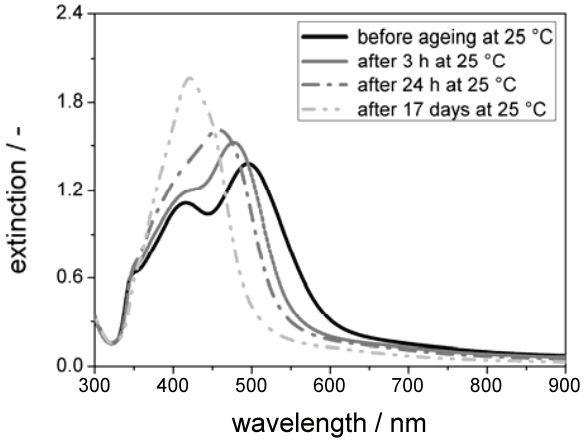

Figure 2: Extinction spectra of aqueous suspensions of rod-like silver particles as a function of ageing time at 25 °C.

During ageing, the shortening of the rods is reflected by the shift of the longitudinal SPR towards shorter wavelengths until after 17 days of ageing at 25 °C only one peak at 415 nm and a small shoulder which can be ascribed to the small and thick "nanobuns" marked in Figure 1D is obtained. For a more quantitative insight the aspect ratio distributions of the silver nanoparticles are derived from the SEM images. Before ageing a mean aspect ratio of about 14 is calculated whereas after 17 days of ageing the aspect ratio decreases down to 3. However, regarding the SEM micrographs in Figure 1A and 1D the intuitional assumption that one nanorod is leading to one spherical particle seems not to be true as the particles become smaller.

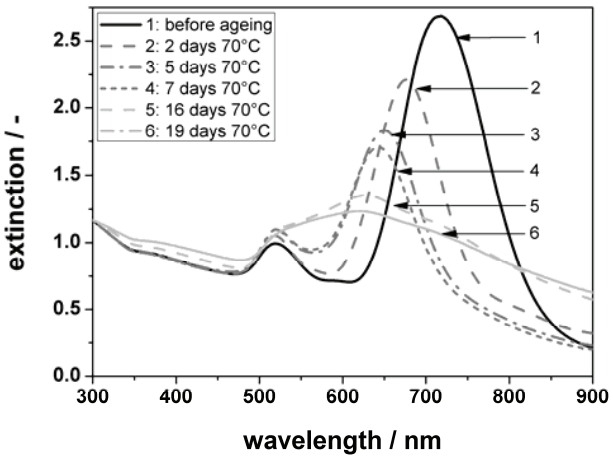

Figure 3: Extinction spectra of aqueous suspensions of rod-like gold particles as a function of ageing time at 70 °C.

In comparison, the gold nanorods show a much larger stability then the silver nanorods as the shape transformation process only starts at elevated temperatures, e.g. at 70 °C. However, a similar change in the absorption behaviour is observed as already seen from the silver nanoparticles. The peak at larger wavelengths of the original, bimodal absorption spectrum shifts towards smaller wavelengths and vanishes.

To obtain a more quantitative insight the suspensions were investigated by anodic stripping voltammetry. With this method dissolved silver ions can be detected down to a lower concentration of 5 µg/l. This corresponds to about 0.006% of the overall silver concentration. However, no silver ions could be detected in the liquid phase after 1 h, 3 h, 24 h or 17 days of ageing at 25 °C, respectively. Thus, the whole amount of silver must be situated in the solid phase and no permanent dissolution of solid can take place. To see how the particle number density changes during ageing, the number density distribution of the volume equivalent sphere is calculated (see Figure 4).

Accordingly, the following assumption has to be fulfilled.

$$m^{A}_{solid} = V^{A}_{solid} \cdot \rho_{Ag} \overset{!}{=} m^{B}_{solid} = V^{B}_{solid} \cdot \rho_{Ag} \qquad (1)$$

The index A refers to the suspension immediately after synthesis and the index B to the suspension after ageing.

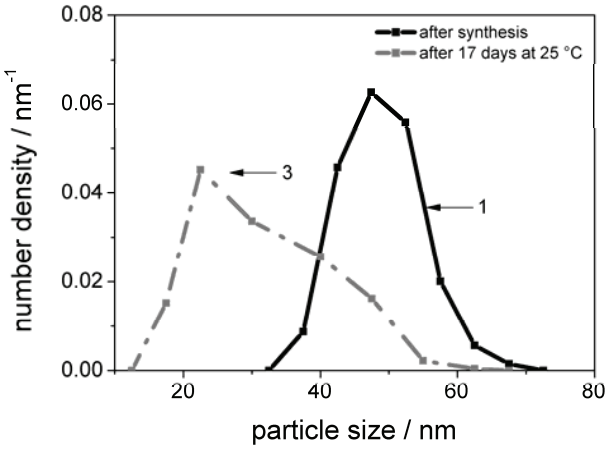

Figure 4: Number density distributions of the silver particles after synthesis (1, black line) and after 17 days (2, orange line) at 25 °C derived from the volume density distributions of the volume equivalent spheres.

Cancelling the density of silver ρ_{Ag} and replacing the overall particle volume by the corresponding number density distributions $q_0^A(x)$ and $q_0^B(x)$, multiplied by the absolute number of particles N^A and N^B and by the volume of each particle size fraction $\frac{\pi}{6}x_i^3$, the following equation 2 is derived.

$$\underbrace{\sum_i \left(x_i^3 \cdot q_0^A(x_i) \cdot \Delta x_i\right)}_{M^A_{3,0}} \cdot N^A \overset{!}{=} \underbrace{\sum_i \left(x_i^3 \cdot q_0^B(x_i) \cdot \Delta x_i\right)}_{M^B_{3,0}} \cdot N^B \qquad (2)$$

The ratio of the particle number density before and after ageing goes reciprocal with the ratio of the third moment of their number density distributions. As the calculation reveals a moment ratio of around 1/3 the number density increases during ageing and the particles must decay.

3.2 Investigation of the nanorods by TEM

From the previous section it can be concluded that there is material transport from surfaces of higher energy to surfaces of lower energy. Different surface energies can be either an intrinsic phenomenon, e.g. regarding gold in the fcc crystal structure, the 111 surface possesses a slightly smaller surface energy than the 100 or the 110 surface, respectively.[6] On the other hand, e.g. regarding silver in the fcc crystal structure, all surfaces, 111, 100 and 110 have about the same intrinsic surface energies.[6] Different surface energies can only be obtained by different surface curvatures, i.e. by varying the particle diameter, or by defects at the particle surface. A careful analysis of the SEM-micrographs of the silver particles shows that during early stages of ripening the diameter of the rods becomes locally smaller (Fig. 1b, particles marked with an arrow). Also a TEM-micrograph of aged gold nanorods (Fig. 5, particles marked with an arrow) reveals that some of the particles got a shape like a "dog-bone".

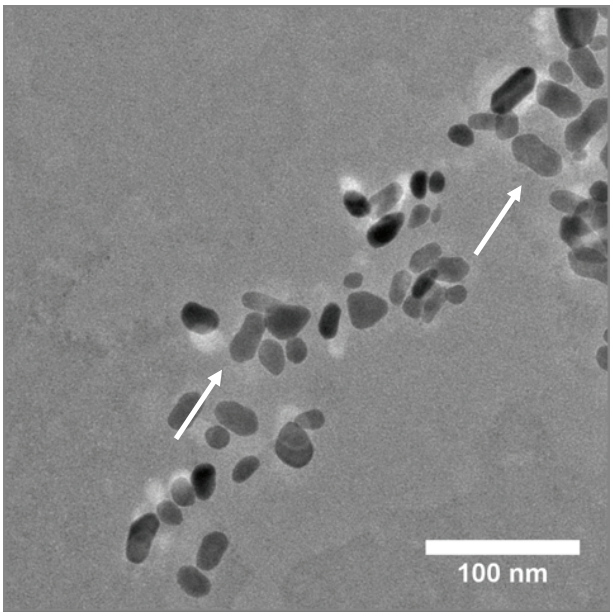

Figure 5: TEM micrograph of "dog-bone" shaped gold nanoparticles after 19 days of ripening at 70 °C.

Consequently, material must have been removed from other areas of the rod leading to a decrease of the rod diameter there. In general, during ripening the rod diameter becomes more and more inhomogeneous until it starts to decay. The calculation above even shows that the particle number increases during ripening. Thus, the rods break in smaller particles. This effect probably depends on the internal five-fold defect structure which leads to defects at the surface which in turn act as "nucleation" centres for fracture during ripening.

4 CONCLUSION

We have demonstrated that during the ageing of aqueous suspensions of rod-like silver and gold nanoparticles at 25 °C or 70 °C, respectively the aspect ratio decreases with time whereas the absolute particle number increases. This was evidenced by anodic stripping voltammetry and general calculations on the particle size distribution. Microscopic investigations showed the appearance of so-called dog-bone structures which are seen to be transition states during the particle decay. Regarding the increased interest in anisotropic nanoparticles during the past years also a control of their long-term stability will be one of the great challenges in nanotechnology.

5 ACKNOWLEDGEMENTS

The authors would like to thank the German Research Council (DFG) for their financial support (Projects PE427/18-2) which supports within the framework of its Excellence Initiative the Cluster of Excellence 'Engineering of Advanced Materials' (www.eam.uni-erlangen.de) at the University of Erlangen-Nuremberg. Furthermore, we thank Dr. Jochen Schmidt and Stefan Romeis for helpful discussion.

REFERENCES

[1] Gans, R., *Ann. Phys*, *342*, 881, **1912**.

[2] (a) Huang, M. H.; Choudrey, A.; Yang, P., *Chem. Commun.*, *12*, 1063; (b) Nikoobakht **2000**; B.; El-Sayed, M. A., *Chem. Mater., 15*, 1957, **2003**; (c) Sau, T. K.; Murphy, C. J., *Langmuir, 20*, 6414, **2004**; (d) Murphy, C. J.; Gole, A. M.; Hunyadi, S. E.; Orendorff, C. J., *Inorg. Chem., 45*, 7544, **2006**; (e) Jana, N. R.; Gearheart, L.; Murphy, C. J., *J. Phys. Chem. B, 105*, 4065, **2001**.

[3] Xia, Y.; Xiong, Y.; Lim, B.; Skrabalak, S., *Angew. Chem. Int. Ed., 48*, 60, **2009**.

[4] (a) Reindl, A.; Peukert, W., *J. Coll. Int. Sci., 325*, 173-178, **2008**; (b) Marczak, R.; Segets, D.; Voigt, M.; Peukert, W., Optimum between purification and colloidal stability of ZnO nanoparticles. *Advanced Powder Technology, DOI: 10.1016/j.apt.2009.10.005,* **2009**.

[5] (a) Jana, N. R.; Gearheart, L.; Murphy, C. J., *Chem. Commun., 7*, 617, **2001**; (b) Murphy, C. J.; Sau, T. K.; Gole, A. M.; Orendorff, C. J., *MRS Bulletin, 30*, 349, **2005**; (c) Sau, T. K.; Murphy, C. J., *Langmuir, 21*, 2923, **2005**.

[6] Vitos, L.; Ruban, A. V.; Skriver, H. L.; Kollár, J., *Surface Science, 411*, 186-202, **1998**.